Release of Isolated Single Kinesin Molecules from Microtubules†

Yuliya Vugmeyster,‡ Elise Berliner,§ and Jeff Gelles*

Department of Biochemistry and The Center for Complex Systems, Brandeis University, Waltham, Massachusetts 02254

Received June 25, 1997; Revised Manuscript Received November 4, 1997⊗

ABSTRACT: Previous studies on the motor enzyme kinesin suggesting that the enzyme molecule tightly binds to a microtubule by only one of its two mechanochemical head domains were performed with multiple kinesin molecules on each microtubule, raising the possibility that interactions between adjacent bound molecules may interfere with the binding of the second head. To characterize the microtubule-bound state of isolated single kinesin molecules, we have measured the rates of nucleotide-induced dissociation of the complex between microtubules and bead-labeled single molecules of the dimeric kinesin derivative K448-BIO using novel single-molecule kinetic methods. Complex dissociation by <2 μM ADP displays an apparent second-order rate constant of 1.2×10^4 M^{-1} s^{-1}. The data suggest that only one of the two heads is bound to the microtubule in the absence of ATP, that binding of a single ADP to the complex is sufficient to induce dissociation, and that even lengthy exposure of kinesin to the microtubule fails to produce significant amounts of a two-head-bound state under the conditions used. The inhibitor adenylyl imidodiphosphate (AMP-PNP) induces stochastic pauses in the movement of bead-labeled enzyme molecules in 1 mM ATP. Exit from pauses occurs at 2 s^{-1} independent of AMP-PNP concentration. The same rate constant is obtained for dissociation of the transient kinesin−microtubule complexes formed in 1 mM ADP, 0.5 mM AMP-PNP, suggesting that release of a single AMP-PNP molecule from the enzyme is the common rate-limiting step of the two processes. The results are consistent with alternating-sites movement mechanisms in which two-head-bound states do not occur in the enzyme catalytic cycle until after ATP binding.

Kinesin and its homologs are motor enzymes that use the free energy derived from ATP hydrolysis to drive the movement of membrane-bounded organelles, chromosomes, and other subcellular structures along cytoplasmic microtubules (*1*). Kinesin is a heterotetramer of two heavy chains and two light chains (*2*−*4*). The N-terminal ∼340 amino acids of each heavy chain form a compact globular "head" domain with dimensions $7 \times 4.5 \times 4.5$ nm (*5*). Studies of truncated heavy chain derivatives demonstrated that the head contains a single ATPase catalytic site (*6*) and is sufficient to generate movement of the enzyme along microtubules (*7, 8*). Kinesin molecules move along the microtubule in discrete 8 nm steps, each of which corresponds to the net hydrolysis of one molecule of ATP (*9*−*12*).

A variety of experimental results demonstrate that kinesin and its two-headed derivatives are "processive" motors that maintain a continuous association with the microtubule for multiple catalytic turnovers and multiple mechanical steps: (i) the ability of kinesin molecules to follow the tracks of microtubule protofilaments during movement (*13*−*16*), (ii) the ability of single kinesin molecules to move continuously for hundreds of nanometers along the microtubule without dissociation (*17*−*20*), (iii) measurements demonstrating that the ATPase $k_{cat}/K_{1/2,microtubule}$ is larger than either the measured rate constant for the kinesin−microtubule association reaction or the calculated maximum diffusion-limited rate constant of that reaction (*21*−*23*), and (iv) demonstration that nucleotide-stimulated release of kinesin from the microtubule is slower than k_{cat} and thus cannot be a step in the turnover cycle (*24, 25*). One-headed derivatives of kinesin generally fail to display these hallmarks of processive movement (*6, 14, 19, 20*), consistent with proposals that a two-headed structure is required for processive movement. [However, there is some evidence for limited processivity of ATP hydrolysis by one-headed derivatives (*23, 26, 27*).]

Movement of kinesin along the microtubule is thought to involve repeated microtubule binding and dissociation by individual kinesin heads, with the binding and dissociation reactions induced by changes in the chemical species bound at the catalytic sites. Heads bind tightly to the microtubule in the absence of nucleotide or in the presence of the substrate analog andenylyl imidodiphosphate (AMP-PNP)[1] [an inhibitor of kinesin motility (*28*)], but much more weakly in the presence of ADP (*2, 29*−*31*). Binding of an ADP molecule and a microtubule to a kinesin head are thus mutually antagonistic.

† Supported by NIH Grant GM43369.

* Address correspondence to this author at the Department of Biochemistry, MS 009, Brandeis University, 415 South St., Waltham, MA 02254. Telephone: 781-736-2377. Email: gelles@binah.cc.brandeis.edu.

‡ Current address: Department of Biology, Massachusetts Institute of Technology, Cambridge, MA 02138.

§ Current address: Intelligent Medical Imaging, Inc., Palm Beach Gardens, FL.

⊗ Abstract published in *Advance ACS Abstracts,* December 15, 1997.

[1] Abbreviations: AMP-PNP, adenylyl imidodiphosphate; BSA, bovine serum albumin.

S0006-2960(97)01534-1 CCC: $15.00
Published on Web 01/13/1998

A major unsolved problem in understanding the mechanistic features that underlie processive kinesin movement is determination of the order and rate constants for all steps in the catalytic cycle and the structures of the reaction intermediates. Important insights into the mechanism have come from comparing the properties of one- and two-headed kinesin derivatives in biochemical and motility experiments. For example, kinesin with ADP bound at the active site rapidly releases nucleotide when the enzyme is mixed with microtubules (*25, 31, 32*). A one-headed derivative can rapidly release essentially all of its bound ADP. In contrast, a two-headed derivative with an ADP molecule bound at each of its two sites releases rapidly only half of its bound ADP molecules; the remaining half releases much more slowly than catalytic turnover. These results suggest the formation of a stable species in which one head is bound to the microtubule and releases nucleotide while the other head is blocked from microtubule binding (presumably by steric constraints) and therefore retains its bound ADP. [In contrast, some data have been interpreted as supporting models in which both kinesin heads bind at least weakly to the microtubule in the absence of added nucleotides (*24, 25, 33*).] The interpretation that each enzyme dimer has only one bound head is consistent with the cryoelectron microscopy reconstructions of complexes between two-headed kinesin derivatives and microtubules (*34, 35*), which also suggest that each dimer has one bound and one free head. The one-head-bound state is an intermediate in hypothesized alternating site mechanisms of kinesin movement (*16, 25, 32*). However, the relevance of the experimental data to the movement mechanism of isolated single kinesin molecules is unclear, as evidence for the state comes entirely from experiments performed under conditions in which multiple kinesin molecules were bound to each microtubule. Under such conditions, interactions between adjacent microtubule-bound kinesin molecules may influence their properties. The structural experiments in particular were performed with microtubules saturated with dimeric kinesin, raising the possibility that the binding of the free head may be blocked by the occupancy of adjacent microtubule lattice positions by the bound heads of other molecules. This mechanism may also explain the substantial effects of changing the fractional saturation of microtubule lattice positions on kinesin pre-steady-state and steady-state ATPase kinetics (*21, 26*). Even the ADP release experiments, which are conducted at much lower kinesin:tubulin ratios, may be influenced by stabilizing interactions between adjacent microtubule-bound enzyme molecules. There is evidence for analogous interactions between microtubule-bound dynein molecules (*36*−*38*). If such interactions are strong, the resultant cooperative binding of kinesin molecules to microtubules will cause most kinesin molecules to occupy lattice sites adjacent to occupied sites, even when experiments are performed at low enzyme:tubulin ratios. In such a system, the measured macroscopic properties of the enzyme will be those of molecules adjacent to (and interacting with) other bound enzyme molecules, not those of the isolated molecules characterized in single-molecule motility experiments.

We here report a characterization of the tightly microtubule-bound states of *isolated individual* molecules of a two-headed kinesin derivative. These states, formed in the absence of added nucleotide or in the presence of AMP-PNP, are putative intermediates (or analogs of intermediates) in the processive motion of kinesin along microtubules. To study their properties, we have examined the kinetics of ADP- or ATP-induced breakdown of the complex between a microtubule and the kinesin derivative K448-BIO. K448-BIO consists of the 448 N-terminal residues of the *Drosophila* kinesin heavy chain linked to 87 residues of the *E. coli* biotin carboxyl carrier protein (BCCP). The BCCP domain is posttranslationally biotinated *in vivo*, facilitating specific labeling of the enzyme with streptavidin conjugates. K448-BIO forms highly stable dimers with steady-state ATPase, processivity, and microtubule-tracking activities similar or identical to those of native kinesin (*14, 20, 39, 40*). The experiments were performed using light microscopy to detect microtubule binding and movement by individual K448-BIO molecules attached to streptavidin-coated microscopic polymer beads. Bead attachment ensures that single enzyme molecules are observed in isolation. In addition, the kinetic measurements on bead-attached molecules are performed under physical and chemical conditions identical to those used for nanometer-resolution motility studies (*9*−*12, 41*); the relevance of the measurements to previously characterized features of the movement mechanism is therefore more certain. The results are consistent with a model in which the enzyme−microtubule complex formed in the absence of added nucleotide has only a single bound head and requires binding of only a single ADP molecule to dissociate and in which AMP-PNP release limits the rate of breakdown of the enzyme/AMP-PNP/microtubule complex in the presence of either ADP or ATP. Our studies support hand-over-hand movement models in which two-head bound states occur in the catalytic cycle only after ATP binding to one head.

MATERIALS AND METHODS

Materials. K448-BIO (*40*) is a biotinated kinesin derivative that consists of the 448 N-terminal residues of the *Drosophila* kinesin α chain, followed by 2 serine residues and the 87 C-terminal residues of the *E. coli* biotin carboxyl carrier protein. K448-BIO was expressed using the baculovirus expression vector system and purified as previously described (*40*). Purified enzyme was stored at 0 °C and used within 4 days, and was centrifuged at 21000*g* for 20 min immediately prior to use. K448-BIO concentration was measured using the Bradford (*42*) assay standardized with bovine serum albumin (BSA; *43*). Microtubules were polymerized from bovine brain tubulin and stabilized with taxol (gift of N. R. Lomax, National Cancer Institute) as described (*43*). Globulin-free BSA and chromatographically purified bovine α-casein were purchased from Sigma.

Streptavidin-Conjugated Beads. Carboxylated polystyrene beads (109 nm diameter) (Seradyn) were conjugated with streptavidin (Molecular Probes) and incubated with 1 mg mL^{-1} BSA and 1 mM dithiothreitol as described by Berliner *et al.* (*14*). Bead suspension concentrations were determined by comparing A_{260} to that of standard dilutions of unconjugated beads. Control experiments showed that A_{260} is proportional to concentration in the absorbance range used and that the proteins present in the conjugated bead samples contribute negligibly to the measured absorbance.

Bead−*Enzyme Complexes*. All experiments were performed with bead−kinesin complexes prepared in 50 mM

imidazole chloride, 50 mM NaCl, 2 mM EGTA, 4 mM $MgCl_2$, 0.03 mM 2-mercaptoethanol, and 0.1% Tween-20, pH 6.7, by mixing a solution containing a measured number of streptavidin-conjugated beads with a solution containing an equal number of K448-BIO molecules (final enzyme concentration typically 2 μg mL^{-1}) and incubating 10 min at 0 °C. At the 1:1 molar ratio of enzyme and beads, ≤27% of the beads will bear two or more enzyme molecules if the molecules are distributed randomly. However, in only a small fraction of these beads are two or more enzyme molecules simultaneously able to interact with the microtubule, since the bead diameter is approximately 10-fold larger than the predicted length of a K448-BIO molecule.

Microscopy. The interaction of the bead−enzyme complexes with microtubules were examined in coverslip flow cells (∼10−15 μL capacity) coated with microtubules, rinsed, coated with casein, and then coated with bovine serum albumin as previously described (*14*); the volumes of all rinses were equal to the capacity of the cell. Cells were then rinsed with 2 cell volumes of ABTB buffer (50 mM imidazole chloride, 50 mM KCl, 2 mM EGTA, 4 mM $MgCl_2$, 20 μM taxol, 0.1 mg mL^{-1} bovine serum albumin, pH 6.7) supplemented with the specified concentration of nucleotide(s). Immediately after preparation, bead−enzyme complexes were diluted >10-fold into fresh ABTB−nucleotide solution, and 1 cell volume of the mixture was introduced into the flow cell. The cells were monitored by video differential interference contrast microscopy at ∼25 °C, and bead binding to, motility along, and/or release from the microtubules was videotaped as described (*14*). In some cases, recordings were transferred to a digital video storage device [as in Schafer *et al*. (*44*)] for subsequent frame-by-frame analysis.

Transient-State Bead Release Experiments. To measure the rate of the release of bound enzyme−bead complexes from immobilized microtubules, a cell prepared as described above with no added nucleotide was incubated ∼5 min to allow the enzyme−bead complexes to bind to the immobilized microtubules. The cell was than washed (over ∼1 min) with 20 μL of ABTB buffer supplemented with the specified concentration of ADP to initiate the release of the enzyme−bead complexes from the microtubules. The beads that were bound to visible microtubules at the cessation of the ADP wash (taken arbitrarily as the zero time point) and were not bound at the end of the video recording (25−35 min later) were cataloged as released beads. Some microtubules detached from the surface and were lost from the field of view during the ADP wash or the subsequent incubation; beads attached to such microtubules were not counted as released beads. The cumulative number of beads released at various time intervals after the zero time point was computed; these data were fit to an exponential reaction progress curve to determine the apparent first-order bead release rate constant.

Equilibrium Bead Release Experiments. An alternate experimental design measured release kinetics of bound enzyme−bead complexes from immobilized microtubules under equilibrium conditions using a microscopic (i.e., single-molecule) kinetics method. Enzyme−bead complexes were introduced into a cell containing immobilized microtubules in ABTB buffer supplemented either with 1.6 μM ADP or with 1 mM ADP, 0.5 mM AMP-PNP and examined by video microscopy. Data were collected from a 35 min recording (1.6 μM ADP sample) or five 30 s recordings (1 mM ADP, 0.5 mM AMP-PNP sample). For each bead observed to diffuse up and bind to the microtubule and later to detach and diffuse away from the microtubule, the duration of the binding event was tabulated. Control samples to which no nucleotides were added showed essentially permanent bead binding with only ∼1% of binding events having duration <10 min, indicating that the shorter events observed in experimental samples were caused by ADP-induced detachment of the K448-BIO molecule from the microtubule rather than spontaneous detachment of the streptavidin-conjugated bead from the enzyme molecule. Beads of 109 nm diameter have a Stokes law diffusion coefficient of 3.9×10^{-8} cm^2 s^{-1} and will therefore diffuse an average distance of 8×10^2 nm in a time interval of 0.19 s. Because this distance is similar to the bead image diameter in the microscope, binding events shorter than 0.19 s cannot reliably be distinguished from simple diffusional encounters in which no binding takes place. Therefore, the experimental data distributions were truncated by excluding events shorter than $t_{min} = 0.19$ s. Control experiments in the presence of a saturating concentration (1 mM) of ADP showed very few binding events, none of which (0 of 12 observations) had durations between 0.19 s and 10 min, demonstrating that the events in this time range detected in experimental samples were due to bead binding to the microtubules induced by the presence of AMP-PNP (1 mM ADP, 0.5 mM AMP-PNP experiments) or by the reduced ADP concentration (1.6 μM ADP experiments). Since ADP at high concentrations dissociates specific kinesin−microtubule interactions, the observed longer events presumably arise from nonspecific sticking of the bead to the surface of the chamber or to a microtubule. Therefore, events of duration >10 min were excluded from the experimental bound-state lifetime distributions.

Steady-State AMP-PNP Pausing Experiments. The breakdown kinetics of the AMP-PNP-inhibited enzyme−microtubule complex were measured under steady-state turnover conditions by examining AMP-PNP-induced pauses in bead movement along microtubules in the presence of a high concentration of ATP. Video recordings of microscope samples prepared in 1 mM ATP supplemented with various concentrations of AMP-PNP were visually examined to detect transient pauses in the movement along microtubules of 130 enzyme−bead complexes. Only events that were both preceded and followed by movement along the microtubule were scored as pauses. For all detected pauses, the exact pause length was determined using hardware and image processing algorithms previously described (*13*). In brief, the image processing techniques were used to determine with nanometer-scale precision the (x, y) coordinates of the bead position in each frame (33 ms duration) of the digitized video recording. Bead positions were corrected for stage drift by subtracting the coordinates of a bead stuck to the coverslip surface in the same video field (*13*). Microtubule orientation was determined, and measured positions were projected onto the microtubule axis as described previously (*14*). Exact pause lengths were determined from the resultant displacement parallel to the microtubule axis vs time records using a discrimination algorithm (see Appendix) and were binned to construct pause length distribution histograms. Pauses could not reliably be detected in a small number of bead

records (6 of 130 total) that contained no significant time intervals in which the bead moved at the velocity (~750 nm s^{-1}) observed in the absence of inhibitor; these records were excluded from the analysis.

In control experiments with 1 mM ATP and no AMP-PNP, pauses of duration greater than 0.23 s were detected in none of 15 beads analyzed. Therefore, pauses of duration >0.23 s detected in the experimental samples were due to the presence of AMP-PNP. Some apparent pauses of duration <0.23 s were detected in the control samples; these presumably arise from experimental noise in the position measurements. Therefore, pauses of duration less than t_{min} = 0.23 s were excluded from the experimental pause length distributions. In order to check that all pauses longer than t_{min} were detected in the initial, visual screening of the video recordings, a sample of eight moving bead records at 1 mM ATP, 0.1−0.5 mM AMP-PNP that had no visible pauses was analyzed by the image processing/pause discrimination procedure. No pauses of duration $>t_{min}$ were detected, confirming the adequacy of the visual screening.

In both experimental samples containing ATP and AMP-PNP and controls that contained ATP only, some beads that appeared bound to microtubules never visibly moved during the experiments (duration 10−30 min). Control and experimental samples contained similar numbers of these nonmotile beads (~3 per ~420 μm^2 microscope field), demonstrating that the nonmotile behavior is not induced by AMP-PNP. We attribute the nonmotile beads to the presence of some inactive enzyme molecules and/or to nonspecific binding of some beads to the microtubule or coverslip surface; data from this population of beads were therefore excluded from the statistical analysis of pause lifetimes.

Analysis of Event Distribution Data. To determine kinetic constants from the experimentally observed distributions of binding event lifetimes (equilibrium binding experiments) or pause lifetimes (steady-state pausing experiments), the Levenberg−Marquardt nonlinear least-squares algorithm was used to fit the binned lifetime distributions to

$$n_i/w_i = (N/\tau)\exp[(t_{min} - t_i)/\tau]$$

(a scaled exponential probability distribution function; *45*), where n_i is the number of events in the ith bin, w_i is the width of the ith bin, N is the total number of observed events included in the distribution, t_{min} is the minimum event length included in the distribution, t_i is the event duration corresponding to the center of the ith bin, and τ is the time constant, which is the only fit parameter. First-order rate constants were calculated by taking the reciprocal of the fit value of τ.

RESULTS

Dissociation of the Kinesin−Microtubule Complex at Limiting Concentrations of ADP. In the absence of nucleotides, kinesin binds microtubules tightly. The addition of ADP releases kinesin from the microtubule, yielding free enzyme with 2 mol of ADP bound per mole of two-headed enzyme. To investigate the properties of isolated kinesin molecules bound to microtubules, we measured the dissociation kinetics of bead-labeled enzyme molecules from surface-immobilized microtubules. The bead−enzyme complexes were constructed so that almost all beads will attach to microtubules through only a single enzyme molecule (see Materials and Methods). Bead−enzyme complexes were first allowed to bind in the absence of added nucleotide to microtubules adsorbed to a glass coverslip. Examination of the coverslip surface by video differential interference contrast microscopy showed extensive binding of the beads to microtubules, as well as some (presumably nonspecific; see Materials and Methods) binding of beads to the surface (Figure 1A). Replacement of the solution bathing the surface with an identical solution supplemented with a low concentration (0.10−0.50 μM) of ADP induced slow release of the enzyme−bead complexes from the surface. After 30 min, many beads associated with microtubules had released from the surface (Figure 1B). Bead release had exponential reaction progress curves (Figure 1C), and the first-order release rate constants derived from such curves were proportional to the ADP concentration (Figure 1D), yielding an apparent second-order rate constant $k_{ADP} = 1.2 \times 10^4$ M^{-1} s^{-1}. This rate constant will in general be smaller than the true rate constant for the bimolecular association of ADP with the bead−enzyme−microtubule complex because only a fraction of ADP binding events will result in observable dissociation of the bead−enzyme complex from the microtubule (see Discussion).

The preceding experiment measured the dissociation kinetics of enzyme−microtubule complexes formed in the absence of nucleotide and aged for ~5 min before the addition of ADP to initiate dissociation. However, the enzyme−microtubule complexes formed during this prolonged incubation may differ from those formed transiently during enzymatic turnover. Hackney (*32*) demonstrated that a dimeric kinesin construct displayed biphasic ADP release when mixed with microtubules—approximately half of the ADP was released within the mixing time (~2 s), but additional ADP was released over several minutes in a reaction too slow to be part of the catalytic cycle. To determine the dissociation kinetics of enzyme−microtubule complexes immediately after their formation, we directly observed the lifetimes of individual binding events between enzyme−bead conjugates and microtubules under conditions of macroscopic chemical equilibrium. In the presence of 1.6 μM ADP, the binding event lifetime distribution is exponential (Figure 2), the result expected when the bound state consists of only a single chemical species (*46*). The distribution decays with a rate constant of 0.019 s^{-1}, which agrees within experimental error to the value predicted by the k_{ADP} (1.2×10^4 M^{-1} s^{-1}) calculated from the data of Figure 1D. This experiment demonstrates that complexes which dissociate shortly after formation display the same release kinetics as those that are aged for several minutes. Taken together, the kinetic measurements on ADP-induced dissociation of the bead−enzyme−microtubule complex are consistent with a simple mechanism in which the complex exists predominantly as a single chemical species, the binding to which of a single ADP per enzyme is sufficient to induce subsequent rapid release of the enzyme from the microtubule. The results exclude models in which two ADP molecules are required for release under the experimental conditions used (see Discussion).

Motility of Single Enzyme Molecules in the Presence of AMP-PNP and ATP. To characterize the kinetic properties of the stable enzyme−microtubule complex formed in the

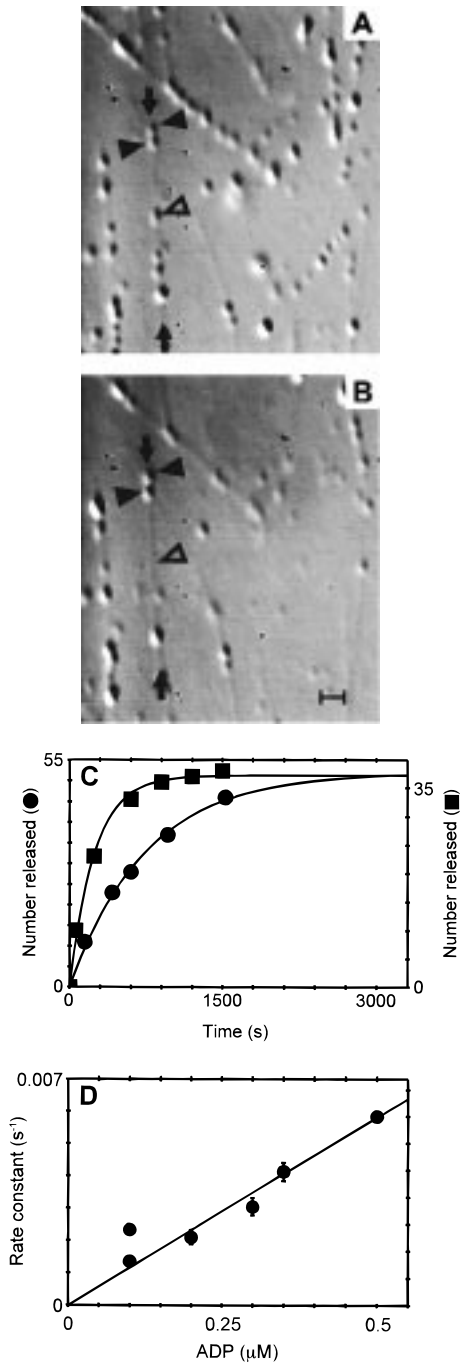

FIGURE 1: Release from microtubules of bead-labeled single K448-BIO molecules induced by low concentrations of ADP. (A, B) Images taken by video-enhanced differential interference contrast light microscopy of microtubules adsorbed to a glass surface and then decorated with bead-labeled kinesin molecules. The images shown are of the same field <0.5 min (A) or 30 min (B) after addition of 3.5×10^{-7} M ADP. On the designated microtubule (arrows), an isolated single bead (open triangle) released from the microtubule during this time interval while other beads (filled triangles) remained bound. Beads also released from other microtubules shown in the field. Scale bar: 1 μm. (C) Total number of beads released from microtubules at a given time after addition of 1.0×10^{-7} M (●) or 3.5×10^{-7} M (■) ADP. Solid lines show exponential fits with apparent first-order rate constants of 1.3×10^{-3} s^{-1} and 4.1×10^{-3} s^{-1}, respectively. (D) Apparent first-order rate constants as a function of ADP concentration (●). Error bars are standard errors; error bars are not shown where bars are smaller than the diameter of the point. The second-order rate constant derived from the slope of fit line is 1.20×10^4 M^{-1} s^{-1} .

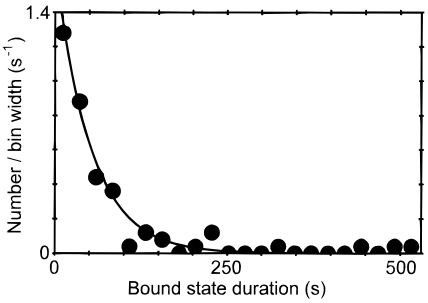

FIGURE 2: Observed microtubule-bound state durations for bead-labeled single K448-BIO molecules in the presence of immobilized microtubules at 1.6 μM ADP. The duration of each observed transient binding event was measured (see Materials and Methods); the graph is a histogram of event durations with the vertical axis scaled by the histogram bin width. Durations from 88 independent binding events are shown; the mean is 71 ± 10 (SE) s. Data were fit to a scaled exponential probability distribution function (—) with a first-order rate constant for exiting the microtubule-bound state of 0.019 ± 0.001 s^{-1}.

presence of the inhibitor AMP-PNP, we first examined under steady-state conditions beads moved along microtubules by single kinesin molecules in the simultaneous presence of AMP-PNP and ATP. Bead movement was studied using an image processing technique that allowed us to measure bead position with nanometer-scale precision with a time resolution of ~30 Hz (*13*). In control experiments containing 1 mM ATP only, beads are seen to move continuously along microtubules: interruptions or pauses in movement with duration >0.23 s are rarely observed (Figure 3A; see Materials and Methods). When AMP-PNP is added, a new behavior is observed: the enzyme−bead conjugates move along microtubules at approximately constant velocity, then abruptly cease moving ("pause") for up to several seconds, and then resume constant-velocity movement. Although 65% of pauses occurred in isolation (Figure 3B), we also sometimes observed a series of pauses separated by only brief intervals of movement. Figure 3C shows the longest recorded example of such a series; the average number of pauses per series over all data records was 2.2. Analysis of a sample of movements occurring in the time intervals between pauses demonstrated that the mean velocity in these intervals [660 ± 48 (SD) nm s^{-1}] is similar to the velocity observed in the absence of AMP-PNP (752 ± 57 nm s^{-1}). In contrast, the number of observed pauses increases as the AMP-PNP concentration is increased from 0.05 to 0.5 mM. These results suggest that induction of the lengthy pauses observed here is the primary means by which AMP-PNP inhibits the movement of single kinesin molecules.

Enzyme molecules exiting a pause could recommence movement along the microtubule at the location at which they stopped moving. Alternatively, the enzyme might detach from the microtubule, diffuse through the solution, and then in some fraction of events resume movement by binding at a new location. The latter mechanism would be expected to result in backward movement at the end of approximately half of the pauses after which movement was successfully resumed. In fact, backward movements >20 nm were seen at the end of only 3 of 58 pauses analyzed. Similarly, displacements perpendicular to the microtubule axis large enough to demonstrate that the enzyme had switched from one microtubule protofilament to another (*13*−

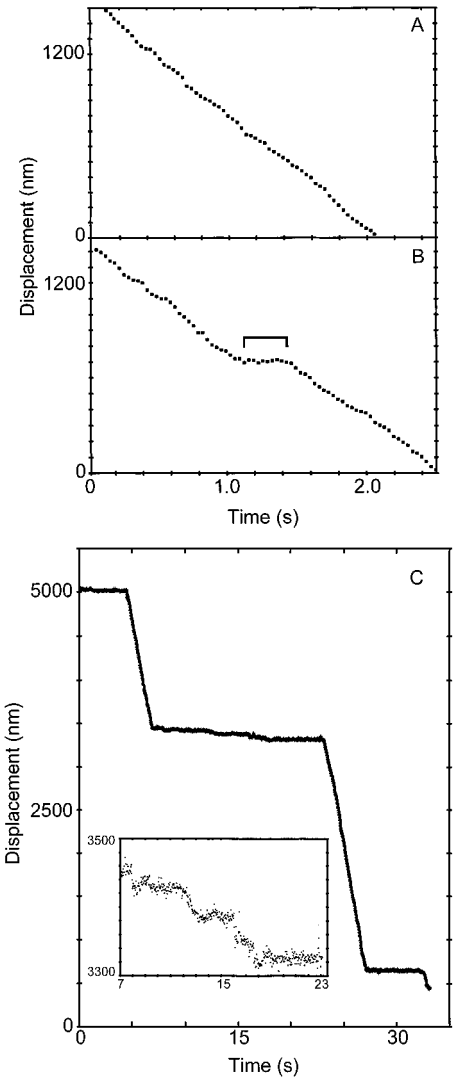

FIGURE 3: Movement of bead-labeled single K448-BIO molecules on immobilized microtubules. Graphs show bead displacement parallel to the microtubule axis as a function of time. Samples contained 50 mM imidazole chloride, 50 mM KCl, 2 mM EGTA, 4 mM $MgCl_2$, 20 μM taxol, and 0.1 mg mL^{-1} bovine serum albumin, pH 6.7, supplemented with either 1 mM ATP (A) or 1 mM ATP and 0.5 mM AMP-PNP (B and C). Note pauses in bead movement in traces B (bracket) and C. Inset: Expansion of trace C in the 7−24 s interval showing multiple short pauses.

16) also were rarely observed. Taken together, these results suggest either that dissociation from the microtubule rarely occurs at the end of the pause or that such dissociations must typically be briefer than the ~4 μs required on average for the bead complex to diffuse 4 nm to the closest binding site on the adjacent microtubule protofilament (calculated from the Stokes law diffusion coefficient of the 109 nm diameter bead, 3.9×10^{-8} cm^2 s^{-1}). To confirm that little or no enzyme−microtubule dissociation occurs from the AMP-PNP-induced pause state, we compared the distance moved by enzyme−bead complexes in the presence and absence of AMP-PNP. The average value of this "run distance" over a sample ($N = 10$) of bead movements in 1 mM ATP [2.3 ± 0.7 (SE) μm] was essentially identical to that obtained in 1 mM ATP, 0.25 mM AMP-PNP (2.2 ± 0.6 μm), demonstrating that no significant increase in the enzyme−microtubule dissociation rate is induced by the inhibitor.

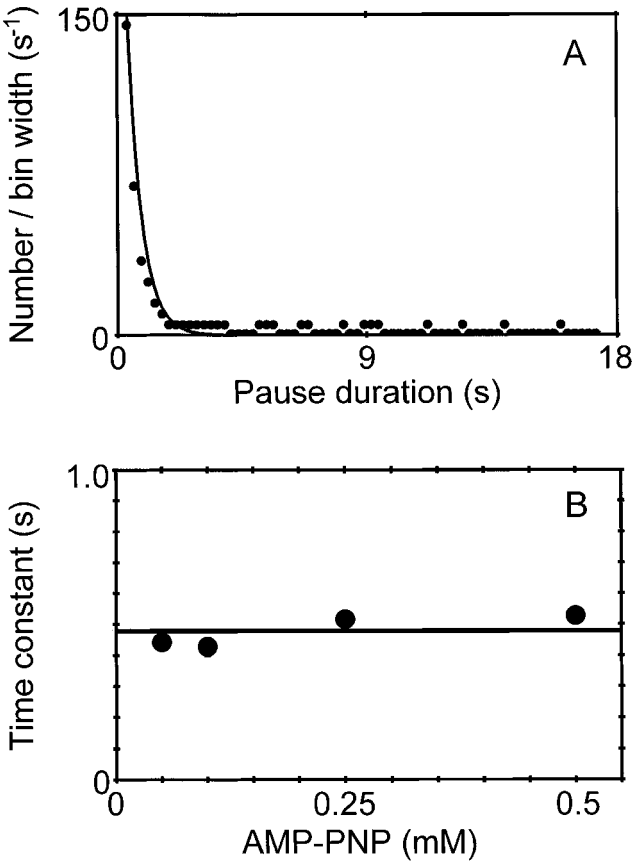

FIGURE 4: Pause durations for bead-labeled single enzyme molecules moving on microtubules in the presence of ATP and AMP-PNP. (A) Histogram of 82 pause durations measured in 1 mM ATP, 0.25 mM AMP-PNP with the vertical axis scaled by the histogram bin width (●). Data were fit to a scaled exponential probability distribution function with time constant 0.52 ± 0.02 s (—). (B) Paused state time constants for enzyme movement in the presence of 1 mM ATP and 0.05, 0.1, 0.25, or 0.5 mM AMP-PNP (●), determined from measurements on $N = 70$, 79, 82 (from A), or 60 pauses, respectively. The mean of the data is 0.48 s (—).

To examine the kinetics of exit from the paused state, we measured the distributions of pause durations at AMP-PNP concentrations from 0.05 to 0.5 mM in the presence of constant 1 mM ATP. In all cases, the distributions were exponential (for example, Figure 4A), consistent with a mechanism in which the paused state is a single chemical species. One possible interpretation of the observations is that the rate of exit from the pause is limited by slow dissociation of AMP-PNP from the enzyme. Consistent with this model, the time constants of the pause duration distributions are independent of AMP-PNP concentration (Figure 4B). The average time constant is 0.48 s, which corresponds to a rate constant for exiting the pause state of 2.1 s^{-1}.

ADP-Induced Dissociation of the AMP-PNP−Enzyme−Microtubule Complex. As an alternative way to characterize the breakdown rate of the AMP-PNP−enzyme complex bound to the microtubule, we also measured the bound complex lifetime at equilibrium in the presence of 0.5 mM AMP-PNP and 1 mM ADP. Control experiments with 1 mM ADP only showed essentially no binding of the enzyme−bead conjugates to microtubules (see Materials and Methods). In contrast, frequent, transient association of the enzyme−bead complexes with microtubules was observed

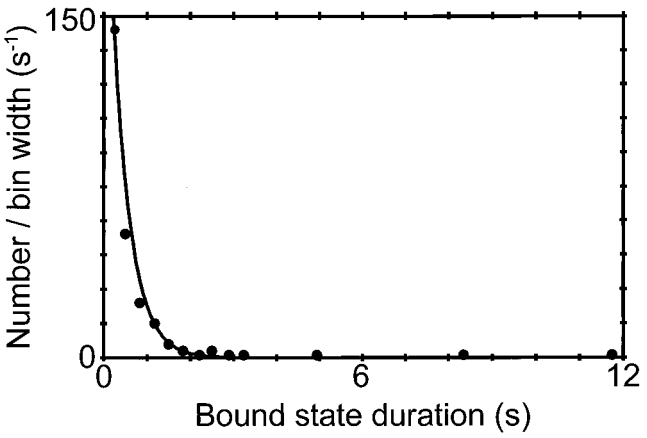

FIGURE 5: Microtubule-bound state duration distribution for bead-labeled single enzyme molecules in 1 mM ADP and 0.5 mM AMP-PNP (●). The graph is a histogram of the durations of 82 binding events, with the vertical axis scaled by the histogram bin width. Histogram bins for durations between 12 and 30 s had number/bin widths less than 0.3 s^{-1} and are not shown. Data were fit to a scaled exponential probability distribution function with time constant 0.41 ± 0.04 s (—).

when AMP-PNP was added along with the ADP. As expected, no movement of the enzyme−bead complexes along the microtubule is observed under these conditions. The measured distribution of the durations of bead−microtubule associations is well fit by a scaled exponential lifetime distribution (Figure 5), again consistent with a microtubule-bound state made up of a single chemical species. The apparent time constant for exiting the microtubule-bound state is 0.41 s, corresponding to a dissociation rate constant of 2.4 s^{-1}. The similarity of this rate constant to the rate constant for exiting the AMP-PNP-induced pause state in the motility experiments suggests that exit from the pause and release of the bound state share a common, rate-limiting step (such as dissociation of AMP-PNP) which results in relief of AMP-PNP inhibition.

DISCUSSION

Microscopic Kinetics. Previous studies used macroscopic (i.e., population averaging) methods, such as light scattering and fluorescence, to analyze the binding and release kinetics of motor enzyme molecules to cytoskeletal filaments. The microscopic (i.e., single-molecule) approach employed here is a useful adjunct to these traditional methods. Macroscopic experiments are frequently performed at high fractional saturation of the filament with enzyme. Under such crowded-binding conditions, adjacent bound enzyme molecules may interact, in which case the observed dissociation kinetics will not be a true reflection of the properties of single enzyme−filament binding. This can be true even at low fractional saturation if enzyme binding is strongly positively cooperative. (The extent of cooperativity in kinesin−microtubule binding has not been reported.) Studies that examined the movement *in vitro* of bead-labeled single kinesin molecules with nanometer-scale precision have provided the most detailed information about the mechanical aspects of the kinesin catalytic cycle (*9*−*12*, *41*). Fuller understanding of kinesin chemomechanical coupling is facilitated by studies which, like those reported here, examine microtubule binding of bead-labeled single molecules, thereby eliminating the possibility that measured release rate constants will differ from those relevant to the motility experiments because of intermolecular interactions between bound enzyme molecules or because the bead slows diffusion of the released enzyme molecule. Bead attachment also makes the diffusion properties of the complex more similar to those *in vivo*, where functioning kinesin molecules are attached to membrane-bounded organelles. Higuchi *et al.* (*47*) recently used a related approach to study the kinetics of force generation by bead-labeled single kinesin molecules.

The time resolution of the microscopic kinetics method for studying enzyme release from microtubules is limited by the average time required for a released bead to diffuse out of the resolution volume of the microscope, ∼190 ms under the conditions used here (see Materials and Methods). This is considerably poorer than the time resolution of macroscopic stopped-flow spectrophotometry instruments, which is typically on the order of 1 ms. However, the time resolution of the microscopic experiment could be improved considerably by using fluorescence microscopy with smaller beads or free dye-labeled enzyme molecules (*19*); the latter would be expected to have diffusional exit times of ∼0.2 ms.

Dissociation of the Bead−Kinesin−Microtubule Complex by ADP. Measurements of the dissociation kinetics of the bead−kinesin−microtubule complex in the presence of subsaturating ADP concentrations by two different methods (Figures 1 and 2) are consistent with a simple mechanism (Scheme 1) in which there is a single species of enzyme−microtubule complex and this species requires binding of only a single ADP molecule per enzyme dimer to induce enzyme−microtubule dissociation.

Scheme 1

$$\mathrm{MT{\cdot}K{\cdot}ADP} + \mathrm{ADP} \underset{k_1}{\overset{k_{-1}}{\rightleftharpoons}} \mathrm{MT} + \mathrm{K{\cdot}ADP_2}$$

In Scheme 1, K represents a dimeric kinesin molecule and MT is a microtubule. Our observations imply that ADP binding with an apparent second-order rate constant $k_{ADP} = k_{-1} = 1.2 \times 10^4$ M^{-1} s^{-1} limits the rate of the combined ADP binding and bead−kinesin release reactions at the low ADP concentrations used here. This rate constant is considerably slower than second-order rate constants for nucleotide binding to kinesin [$\geq 1.1 \times 10^6$ M^{-1} s^{-1} for MANT-ADP binding to microtubule-bound dimeric human kinesin derivative K379, for example (*48*)]. This suggests that the kinesin−microtubule−ADP complex partitions between competing reactions that release ADP or release the microtubule, with the large majority doing the former. Jiang and Hackney (*26*) measured the rate constant for ADP-induced dissociation of the monomeric DHK357−microtubule complex in solution to be 4.1×10^5 M^{-1} s^{-1}, over 30-fold faster than we observe. While some of this discrepancy might be ascribed to differences between the interactions of monomeric or dimeric constructs with the microtubule (*25*, *30*) or different experimental conditions, most undoubtedly arises from the reduced rotational and translational diffusion rates of the bead-bound kinesin molecules and immobilized microtubules in our experiments. Lowering the diffusion rates increases the probability that thermally severed non-covalent interactions between kinesin and the microtubule

will re-form before the partners can diffuse away from each other, thus decreasing the fraction of ADP binding events that lead to observable kinesin−microtubule dissociation. [An analogous effect of diffusion was previously proposed to explain the differences in dissociation rates observed in various motility assays under steady-state turnover conditions (*18, 19*).] The discrepancy between the kinetics observed with free and bead-labeled molecules underscores the importance of performing measurements of reaction kinetics under physical conditions identical to those used in motility assays if the rate constants from the former are to be used to interpret the mechanisms of movements observed in the latter.

As a kinesin dimer has two active sites, it is also reasonable to consider the mechanism in which consecutive binding of two ADP molecules is required to dissociate the kinesin−microtubule complex (Scheme 2).

Scheme 2

$$\mathrm{MT{\cdot}K} + \mathrm{ADP} \underset{k_4}{\overset{k_{-4}}{\rightleftharpoons}} \mathrm{MT{\cdot}K{\cdot}ADP}$$

$$\mathrm{MT{\cdot}K{\cdot}ADP} + \mathrm{ADP} \underset{k_1}{\overset{k_{-1}}{\rightleftharpoons}} \mathrm{MT} + \mathrm{K{\cdot}ADP_2}$$

In general, Scheme 2 predicts a quadratic dependence of the rate of kinesin−microtubule dissociation on ADP concentration whereas the data of Figure 1D show a linear dependence. To test whether there are any conditions under which Scheme 2 is consistent with the experimental data, we used kinetic simulations (not shown) to examine systematically the behavior of the mechanism for different values of k_{-1}, k_4, and k_{-4}. (There is no need to consider a nonzero k_1 since binding of free kinesin to the microtubules is detected directly in the single-molecule experiments reported here and thus does not reduce the measured dissociation rates as in the case of a macroscopic experiment.) The combination of transient state and equilibrium microscopic kinetics studies reported here serves as a stringent test of Scheme 2 because the initial microtubule-bound species formed in the two types of experiments would be different (MT·K in the former, MT·K·ADP in the latter). The simulation results demonstrate that Scheme 2 is inconsistent with the experimental data (Figures 1 and 2) for nearly all values of the rate constants, assuming that k_{-4} and k_{-1} are $\leq 1.1 \times 10^6$ M^{-1} s^{-1} (*48*). This includes cases where $k_{-4} \gg k_{-1}$ or $k_{-1} \gg k_4$ because such values cannot simultaneously satisfy the constraints imposed by both the equilibrium and transient-state data. The only cases in which Scheme 2 is not excluded by the experimental data are those for which k_{-4}/k_4 is so large ($\gg 10^7$ M^{-1}) that there would be no significant population of MT·K even at the lowest ADP ($\ll$50 nM) concentrations used in the experiments. Thus, the data suggest that only a single ADP molecule is required to dissociate kinesin−microtubule complexes, with the possible exception of complexes formed under conditions in which free ADP has been reduced to extremely low (nanomolar) concentrations.

The conclusion that only a single ADP molecule is required to release bound kinesin from microtubules is consistent with previous studies of the structure and biochemistry of kinesin−microtubule complexes. Electron microscopy on microtubules decorated with dimeric kinesin derivatives reveals that only one of the two heads contacts the microtubule (*34, 35*), suggesting that ADP binding to the bound head is likely to be sufficient to induce release. Only one of the two bound ADP molecules was rapidly released upon binding of a dimeric kinesin construct to microtubules (*25, 31, 32*), suggesting that only one of the two heads interacts strongly with the microtubule and releases ADP, while the other head retains its bound nucleotide (Figure 6B). Consistent with our results, such a structure would have only one vacant nucleotide binding site and thus requires only a single ADP to dissociate (Figure 6, reaction −1). It is possible that the head that retains bound ADP interacts weakly or transiently with the microtubule (*25, 30*). Such a model is consistent with our results providing that weak head binding does not substantially limit release kinetics under the conditions studied here.

Previous studies do not exclude the possibility that a two-head-bound state (e.g., that shown in Figure 6E) is slowly formed upon prolonged incubation of kinesin with microtubules. Steric interactions between adjacent kinesin molecules might preclude formation of such a species when microtubules are densely packed with kinesin, as in the electron microscopy studies. Some measurements of microtubule-induced ADP release (*32*) showed evidence of slow release of the remaining ADP following the initial rapid release of 1 mol of ADP per mole of enzyme dimer. However, our studies show that even slow formation of a species that subsequently requires two ADP molecules for release is unlikely. Kinesin−microtubule complexes formed only briefly in the equilibrium experiment (Figure 2) show identical release kinetics to those subjected to a lengthy preincubation prior to the transient-state release experiment (Figure 1). Thus, formation of a two-head-bound species like that shown in Figure 6E is unlikely under our experimental conditions. We speculate that the slow phase of ADP release observed previously might instead be due to transient detachment of the one-head-bound kinesin dimer (Figure 6B) from the microtubule followed by binding to the microtubule of the head that still retains ADP. This would produce a structure (not shown in Figure 6) with one bound head but no nucleotide which would be expected to display release kinetics similar to the species shown in Figure 6B.

Inhibition of Kinesin Movement by AMP-PNP. Previous quantitative studies of AMP-PNP inhibition of kinesin movement are difficult to interpret mechanistically because they examined only movements induced by multiple kinesin molecules (*28*). Our observation of a monoexponential lifetime distribution for AMP-PNP-induced pauses in the motility of single kinesin molecules is consistent with the formation of a single inhibited enzyme species. While AMP-PNP could in principle bind at any point in the catalytic cycle at which at least one of the two active sites is unoccupied, we propose in Figure 6 a minimal mechanism in which AMP-PNP competes with ATP for binding to the enzyme species (Figure 6B) thought to be the starting point for productive ATP hydrolysis. Such a model is consistent with the observed pause durations if AMP-PNP release controls the rate of exit from a pause [$k_{-2} = \sim 2$ s^{-1}, the reciprocal of the measured pause lifetime; in contrast, k_3 [ATP] is by definition equal to or faster than the k_{cat} of 38 s^{-1} (*12*) at

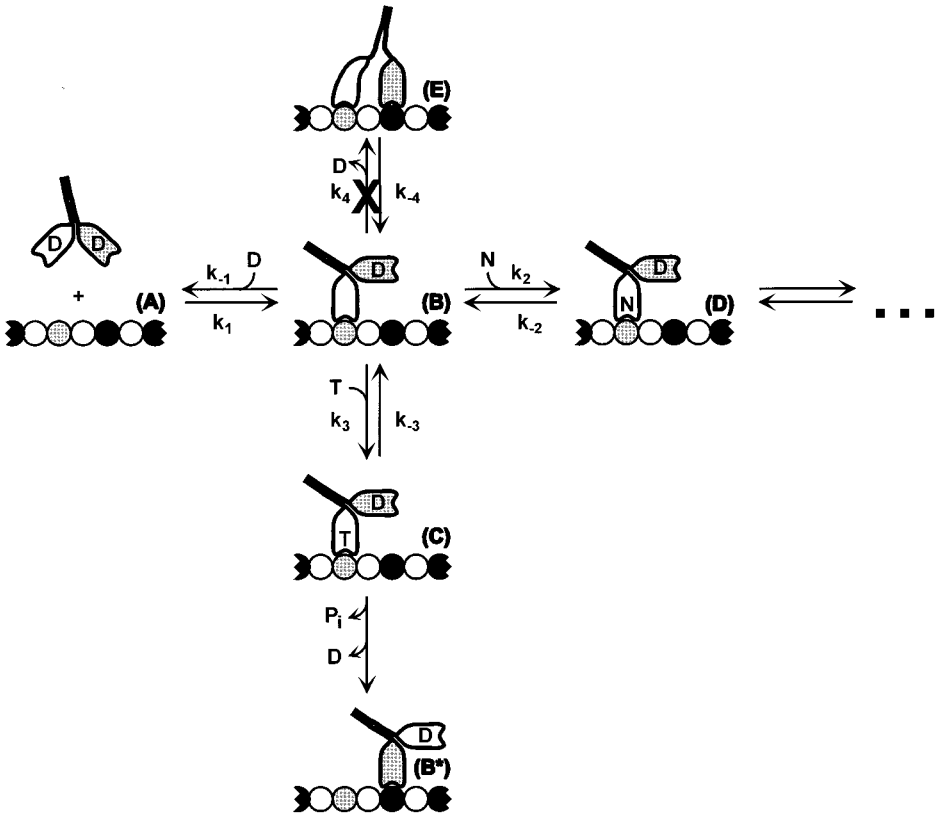

FIGURE 6: Proposed mechanism of kinesin−microtubule interactions. D, ADP; T, ATP; N, AMP-PNP. The row of alternating white and black circles represents the α and β tubulin subunits of a microtubule protofilament. One head of the kinesin molecule is white and the other is shaded gray for identification. A free kinesin molecule with an ADP bound to each head (A) binds to the microtubule to produce a one-head-bound species (B) with concomitant release of one ADP molecule. Subsequent formation of a two-head-bound species (E) does not occur in the absence of nucleoside triphosphates. However, in the presence of either AMP-PNP or ATP, the nucleotide binds to the bound head, initially producing a one-head-bound species (D or C, respectively). In the ATP case, species C subsequently forms a two-head-bound species (not shown) similar in structure to E; detachment of the white head from the microtubule then leads to species B*. These reactions are accompanied by release of ADP from the gray head and by ATP hydrolysis and release of P_i by the white head. The reaction path from B to B* represents a complete catalytic cycle of the microtubule-bound enzyme. The results presented are consistent with the minimal mechanism shown, but they do not rule out formation of a two-head-bound species from species D in the presence of AMP-PNP (ellipsis).

saturating ATP concentrations]. It is also consistent with the observed invariance of pause durations with respect to changes in AMP-PNP concentration. This is because the data require that k_3 must be significantly greater than k_2 (Figure 6), since many ATPase turnovers occur for each AMP-PNP-induced pause when AMP-PNP and ATP are present at similar concentrations. For example, in the experiments in 1 mM ATP, 0.25 mM AMP-PNP, enzyme−bead complexes moved a total distance of ∼360 μm, corresponding to $\sim 4.6 \times 10^4$ 8-nm steps, but paused only $\sim 1.2 \times 10^2$ times. (The latter number includes the 82 observed pauses plus 41 additional pauses estimated from the fit curve in Figure 4 to have occurred with durations shorter than the experimental detection limit of 0.23 s.) k_3/k_2 must therefore be at least 93, demonstrating that AMP-PNP is only a poor kinetic competitor for ATP binding to the rigor enzyme−microtubule complex. The value given is only a lower limit for k_3/k_2 since not all ATP binding events result in turnover in the general case where k_{-3} (Figure 6) may be nonzero.

In the proposed model, the species formed upon AMP-PNP dissociation (Figure 6B) is identical to that (discussed earlier) which can be released from the microtubule by binding a single ADP molecule. Thus, the model is consistent with the observation that the lifetime of the microtubule-bound state in the presence of 1 mM ADP, 0.5 mM AMP-PNP (Figure 5) is identical to the lifetime of the paused state observed in the presence of various concentrations of AMP-PNP and saturating (1 mM) ATP (Figure 4), as long as the rate of the former process is also limited by the rate of AMP-PNP release ($k_{-2} = \sim 2\ s^{-1}$). The apparent rate constant measured for release of bound kinesin induced by micromolar concentrations of ADP ($k_{ADP} = k_{-1} = 1.2 \times 10^4\ M^{-1}\ s^{-1}$) is consistent with this requirement, as it predicts that release of the species in Figure 6B can occur at a rate of up to 12 s^{-1} at 1 mM ADP. Thus, the model of Figure 6 is consistent with all experimental data. However, it should be noted that the data do not exclude certain more complex models, such as ones in which two AMP-PNP molecules are bound by the kinesin−microtubule complex and/or ones in which AMP-PNP binding induces the formation of a two-head-bound state.

The dissociation of AMP-PNP from the enzyme−microtubule complex with the measured rate constant $k_{-2} = \sim 2\ s^{-1}$ converts one microtubule-bound state of the enzyme (Figure 6D) to another (Figure 6B). Therefore, the value of k_{-2}, in contrast to that of k_{-1}, is expected to be independent of the diffusion coefficient of the enzyme. The value

of k_{-2} reported here is thus applicable not only to experiments with enzyme attached to slowly diffusing beads but also to conventional biochemical studies with free enzyme molecules.

Cohn *et al.* (*28*) reported continuous microtubule gliding at submaximal velocities in assays with mixtures of ATP and AMP-PNP. Our nanometer resolution measurements suggest that these submaximal velocities were produced by individual kinesin molecules alternating on a time scale much slower than turnover between an inhibitor-free state that moves along the microtubule at maximal velocity and an inhibited state that does not move at all. In contrast to our data showing that relief of AMP-PNP inhibition of K448-BIO by millimolar concentrations of ADP or ATP occurs within ~2 s, Schnapp *et al.* (*49*) observed that microtubules bound to a surface coated with squid kinesin took 1−2 min to resume movement after exposure to ATP. In that study, the observed microtubule movements were driven by multiple kinesin molecules, and the slow kinetics may arise from the fact that AMP-PNP release must occur from most or all of these molecules before movement can be observed. It is also possible that AMP-PNP, kinesin, and microtubules in the absence of competing nucleotide form an unusually stable complex that takes minutes to dissociate. This possibility is not addressed by our experiments, all of which studied AMP-PNP inhibition in the presence of millimolar concentrations of ATP or ADP.

Implications for the Kinesin Catalytic Cycle. The experiments described here differ from previous studies of the kinetics of kinesin interactions with nucleotides and microtubules in that they were performed with isolated, single kinesin molecules. Thus, the enzyme−microtubule complexes studied here lack the possible kinesin−kinesin interactions and steric constraints to kinesin−microtubule interactions present in earlier studies. Nevertheless, the results presented here are fully consistent with the alternating site mechanisms for kinesin movement along microtubules coupled to ATP hydrolysis that were stimulated by previous solution kinetic studies. In particular, the conclusion that only one molecule of ADP is required to dissociate the kinesin−microtubule complex formed in the absence of ATP provides a new independent line of evidence suggesting that in such complexes only one of the kinesin heads is bound to the microtubule (Figure 6B). The assumption that it is this species which binds ATP and its analogs is consistent with the AMP-PNP experiments, which suggest that pauses are due to slow AMP-PNP release from a species (e.g., that in Figure 6D) that is produced by binding of the inhibitor to the species of Figure 6B. Catalytic turnover initiated by binding of ATP to this same species (Figure 6, reaction 3) would then proceed, presumably through an intermediate in which both heads are transiently bound to the microtubule, to a species (Figure 6B*) identical in structure to the starting complex except that the two heads have swapped roles and the enzyme has advanced one tubulin dimer along the microtubule protofilament. This proposal is consistent with the observed coupling of one 8 nm step to the hydrolysis of each ATP molecule (*11*, *12*). In such a catalytic cycle, both heads of the enzyme are never simultaneously released from the microtubule, leading to the processive movement and protofilament tracking observed of intact kinesin and its dimeric derivatives.

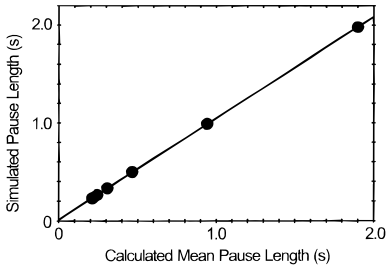

FIGURE 7: Performance of the pause discrimination algorithm on simulated data (●). The graph shows the known pause lengths used in the simulations ("simulated pause length") plotted against the mean length of the pauses as measured by the discrimination algorithm ("calculated mean pause length") for six simulated data records.

ACKNOWLEDGMENT

We gratefully acknowledge the technical assistance of Hansraj Mahtani. We thank Edgar Young and Wei Hua for comments on the manuscript.

APPENDIX: PAUSE DISCRIMINATION ALGORITHM

Nanometer-scale motion analysis of kinesin-driven bead movements produces records of the bead position projected along the microtubule axis as a function of time (for example, Figure 3). Reliable detection and objective measurement of the durations of AMP-PNP-induced pauses in bead movement were accomplished using the following algorithm: Data records were smoothed using a three-point mean filter, and the time derivative of the smoothed data was calculated. The derivative typically had a bimodal distribution with points near 750 nm s^{-1} (the average bead velocity observed in the absence of AMP-PNP) during intervals of bead movement and points near 0 nm s^{-1} during pauses. A two-threshold procedure was applied to the derivative data to detect and measure pauses; upper and lower thresholds were 400 and 150 nm s^{-1}. Any contiguous set of points that contained no points above the upper threshold, but was immediately preceded and followed by points above the upper threshold, was deemed to be a pause. The pause length was calculated as $i(l + m/2)$, where i is the time interval between points and l and m are the number of points within the pause below and above, respectively, the lower threshold.

To verify that the pause discrimination algorithm reliably detected pauses and accurately measured their lengths, we applied the algorithm to simulated data records containing pauses of known lengths. Each simulated data set contained 100 pauses of equal lengths separated by intervals of movement at a constant velocity of 700 nm s^{-1}; the duration of the movement intervals was 1.5 times the pause length. The effect of experimental noise was simulated by adding to these data sets Gaussian-distributed noise with a standard deviation of 6.91 nm, the root-mean-square noise in the experimental data (which was measured as described below). Application of the pause discrimination algorithm to the simulated data sets demonstrated that 100% of pauses were detected for pause lengths ranging from 0.23 s (the shortest pauses included in the experimental data; see Materials and Methods) to 1.98 s. Conversely, the algorithm found no pauses of duration >0.23 s in control simulated data sets in which no pauses were included. Comparison of the mean

pause lengths measured by the algorithm to the actual lengths of the pauses in the simulations showed that the algorithm slightly underestimated the pause lengths (Figure 7). Therefore, reported data derived from the algorithm were corrected for this underestimate by applying the equation for the calibration fit line shown in Figure 7.

The root-mean-square noise in the experimental data was estimated in five bead displacement records from samples containing 1 mM ATP and no AMP-PNP. Each record was fit to a line, and the residual (the difference between the fit line and the experimental data), v_i, was calculated for each point in the record. The root-mean-square noise was then calculated (*50*) as

$$\left\{\frac{\sum_{i=1}^{N-1}(v_i - v_{i+1})^2}{2(N-1)}\right\}^{1/2}$$

where N is the total number of points in the record. The magnitude of the root-mean-square noise used in the simulations (6.91 nm) was the median of the values determined from the five data records analyzed.

REFERENCES

1. Moore, J. D., and Endow, S. A. (1996) *Bioessays 18*, 207−219.
2. Vale, R. D., Reese, T. S., and Sheetz, M. P. (1985) *Cell 42*, 39−50.
3. Bloom, G. S., Wagner, M. C., Pfister, K. K., and Brady, S. T. (1988) *Biochemistry 27*, 3409−3416.
4. Kuznetsov, S. A., Vaisberg, E. A., Shanina, N. A., Magretova, N. N., Chernyak, V. Y., and Gelfand, V. I. (1988) *EMBO J. 7*, 353−356.
5. Kull, F. J., Sablin, E. P., Lau, R., Fletternick, R. J., and Vale, R. D. (1996) *Nature 380*, 550−555.
6. Huang, T. G., and Hackney, D. D. (1994) *J. Biol. Chem. 269*, 16493−16501.
7. Yang, J. T., Saxton, W. M., Stewart, R. J., Raff, E. C., and Goldstein, L. S. B. (1990) *Science 249*, 42−47.
8. Stewart, R. J., Thaler, J. P., and Goldstein, L. S. B. (1993) *Proc. Natl. Acad. Sci. U.S.A. 90*, 5209−5213.
9. Svoboda, K., Schmidt, C. F., Schnapp, B. J., and Block, S. M. (1993) *Nature 365*, 721−727.
10. Coppin, C. M., Finer, J. T., Spudich, J. A., and Vale, R. D. (1996) *Proc. Natl. Acad. Sci. U.S.A. 93*, 1913−1917.
11. Schnitzer, M. J., and Block, S. M. (1997) *Nature 388*, 386−390.
12. Hua, W., Young, E., Fleming, M., and Gelles, J. (1997) *Nature 388*, 390−393.
13. Gelles, J., Schnapp, B. J., and Sheetz, M. P. (1988) *Nature 331*, 450−453.
14. Berliner, E., Young, E. C., Anderson, K., Mahtani, H. K., and Gelles, J. (1995) *Nature 373*, 718−721.
15. Ray, S., Meyhoefer, E., Milligan, R. A., and Howard, J. (1993) *J. Cell Biol. 121*, 1083−1093.
16. Gelles, J., Berliner, E., Young, E. C., Mahtani, H. K., Perez-Ramirez, B., and Anderson, K. (1995) *Biophys. J. 68*, 276s−282s.
17. Howard, J., Hudspeth, A. J., and Vale, R. D. (1989) *Nature 342*, 154−158.
18. Block, S. M., Goldstein, L. S. B., and Schnapp, B. J. (1990) *Nature 348*, 348−352.
19. Vale, R. D., Funatsu, T., Pierce, D. W., Romberg, L., Harada, Y., and Yanagida, T. (1996) *Nature 380*, 451−453.
20. Young, E. C., and Gelles, J. (1997) *Biochemistry* (submitted for publication).
21. Hackney, D. D. (1994) *J. Biol. Chem. 269*, 16508−16511.
22. Hackney, D. D. (1995) *Nature 377*, 448−450.
23. Jiang, W., Stock, M. F., Li, X., and Hackney, D. D. (1997) *J. Biol. Chem. 272*, 7626−7632.
24. Gilbert, S. P., Webb, M. R., Brune, M., and Johnson, K. A. (1995) *Nature 373*, 671−676.
25. Ma, Y. Z., and Taylor, E. W. (1997) *J. Biol. Chem. 272*, 724−730.
26. Jiang, W., and Hackney, D. D. (1997) *J. Biol. Chem. 272*, 5616−521.
27. Ma, Y. Z., and Taylor, E. W. (1997) *J. Biol. Chem. 272*, 717−723.
28. Cohn, S. A., Ingold, A. L., and Scholey, J. M. (1989) *J. Biol. Chem. 264*, 4290−4297.
29. Brady, S. T. (1985) *Nature 317*, 73−75.
30. Rosenfeld, S. S., Rener, B., Correia, J. J., Mayo, M. S., and Cheung, H. C. (1996) *J. Biol. Chem. 271*, 9473−9482.
31. Crevel, I. M. T. C., Lockhart, A., and Cross, R. A. (1996) *J. Mol. Biol. 257*, 66−76.
32. Hackney, D. D. (1994) *Proc. Natl. Acad. Sci. U.S.A. 91*, 6865−6869.
33. Harrison, B. C., Marchese-Ragona, S. P., Gilbert, S. P., Cheng, N., Steven, A. C., and Johnson, K. A. (1993) *Nature 362*, 73−75.
34. Hirose, K., Lockhart, A., Cross, R. A., and Amos, L. A. (1996) *Proc. Natl. Acad. Sci. U.S.A. 93*, 9539−9544.
35. Arnal, I., Metoz, F., DeBonis, S., and Wade, R. (1996) *Curr. Biol. 6*, 1265−1270.
36. Moss, A. G., Sale, W. S., Fox, L. A., and Witman, G. B. (1992) *J. Cell Biol. 118*, 1189−200.
37. Haimo, L. T., and Rosenbaum, J. L. (1981) *Cell. Motil. 1*, 499−515.
38. Takahashi, M., and Tonomura, Y. (1978) *J. Biochem. (Tokyo) 84*, 1339−1355.
39. Berliner, E. (1995) Ph.D. Thesis, Brandeis University.
40. Young, E. C., Berliner, E., Mahtani, H. K., Perez-Ramirez, B., and Gelles, J. (1995) *J. Biol. Chem. 270*, 3926−3931.
41. Svoboda, K., and Block, S. M. (1994) *Cell 77*, 773−784.
42. Bradford, M. M. (1976) *Anal. Biochem. 72*, 248−254.
43. Berliner, E., Mahtani, H. K., Karki, S., Chu, L. F., Cronan, J. E., Jr., and Gelles, J. (1994) *J. Biol. Chem. 269*, 8610−8615.
44. Schafer, D. A., Gelles, J., Sheetz, M. P., and Landick, R. (1991) *Nature 352*, 444−448.
45. Colquhoun, D., and Sigworth, F. J. (1983) in *Single channel recording* (Sakmann, B., and Neher, E., Eds.) pp 191−263, Plenum, New York.
46. Colquhoun, D., and Hawkes, A. G. (1983) in *Single channel recording* (Sakmann, B., and Neher, E., Eds.) pp 135−175, Plenum, New York.
47. Higuchi, H., Muto, E., Inoue, Y., and Yanagida, T. (1997) *Proc. Natl. Acad. Sci. U.S.A. 94*, 4395−4400.
48. Ma, Y.-Z., and Taylor, E. W. (1995) *Biochemistry 34*, 13242−13251.
49. Schnapp, B. J., Crise, B., Sheetz, M. P., Reese, T. S., and Khan, S. (1990) *Proc. Natl. Acad. Sci. U.S.A. 87*, 10053−10057.
50. Bershad, N. J., and Rockmore, A. J. (1984) *IEEE Trans. Inform. Theory*, 112−113.

BI971534O